

11

Plasmonic materials

Figures

11.2 Real metals

11.2.1 Observability function

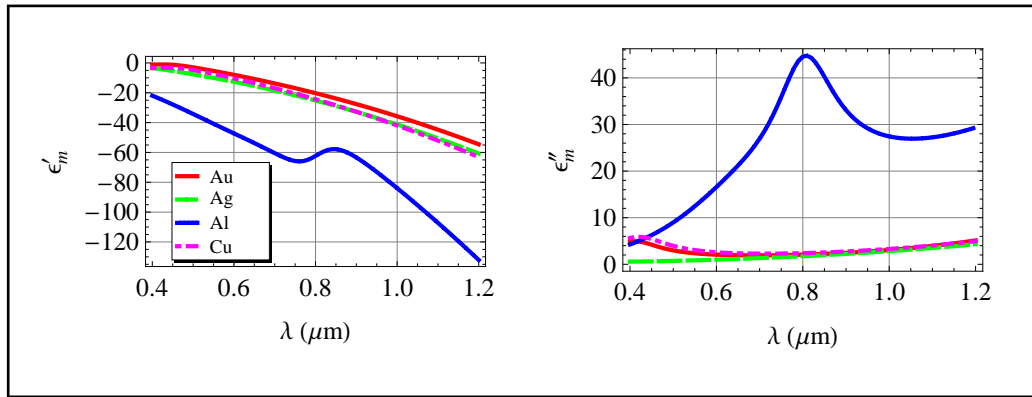


Fig. 11.1. (Left) ϵ'_m and (right) ϵ''_m as a function of wavelength, λ , in the visible and near infrared for the plasmonic metals gold (solid line), silver (long dashes), aluminum (dots) and copper (dot dashes). (*Mathematica* simulation.)

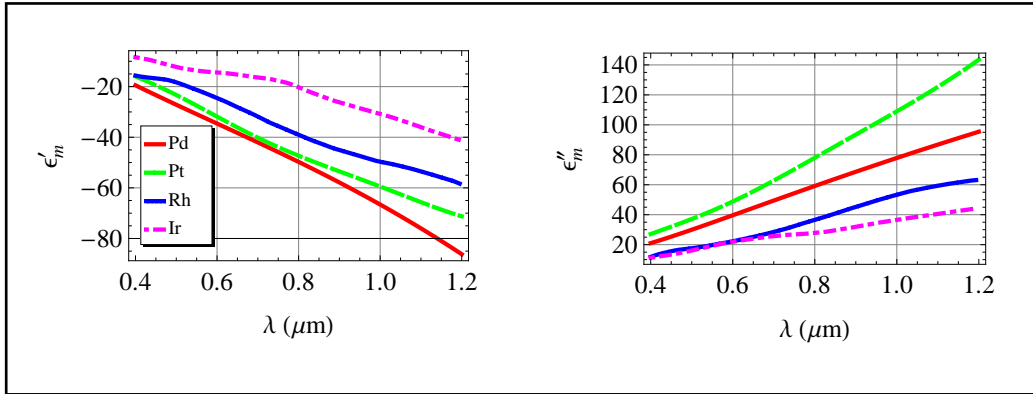


Fig. 11.2. (Left) ϵ'_m and (right) ϵ''_m as a function of wavelength, λ , in the visible and near infrared for palladium (solid line), platinum (long dashes), rhodium (dots) and iridium (dot dashes). (*Mathematica* simulation.)

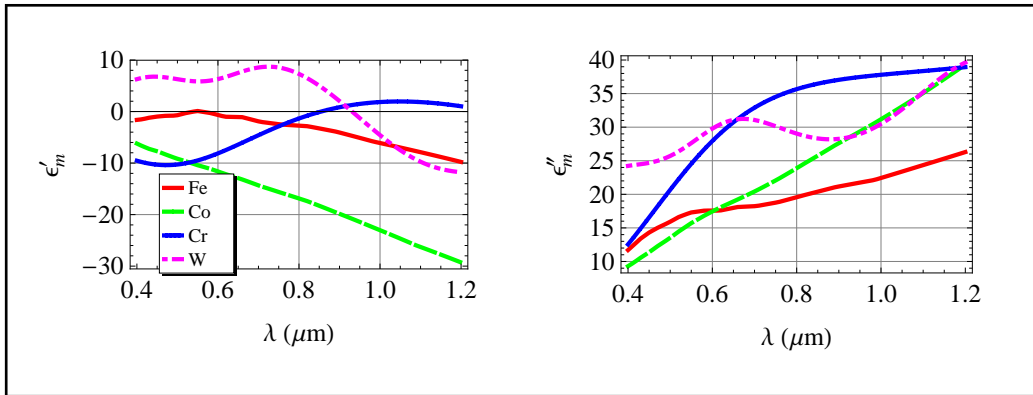


Fig. 11.3. (Left) ϵ'_m and (right) ϵ''_m as a function of wavelength, λ , in the visible and near infrared for iron (solid line), cobalt (long dashes), chromium (dots) and tungsten (dot dashes). (*Mathematica* simulation.)

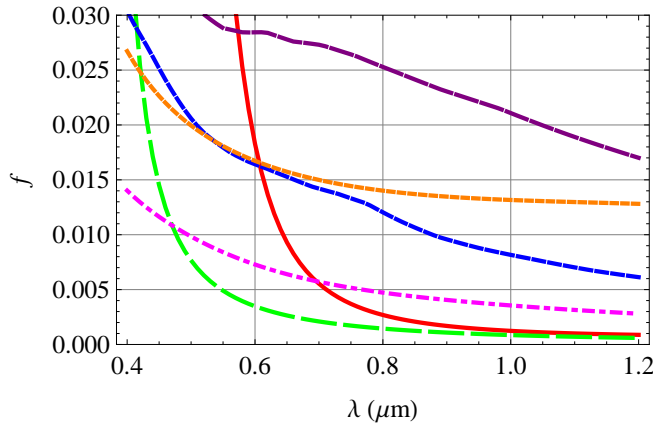


Fig. 11.4. The observability function is plotted as a function of wavelength, λ , for plasmonic metals gold (solid line) and silver (long dashed), for nonplasmonic noble metals platinum (dot dashed) and iridium (short dashes) and transition metals iron (medium dashes) and chromium (dotted). Smaller values of f indicate the metal has greater plasmonic properties. (*Mathematica* simulation.)

11.2.2 Kretschmann resonance

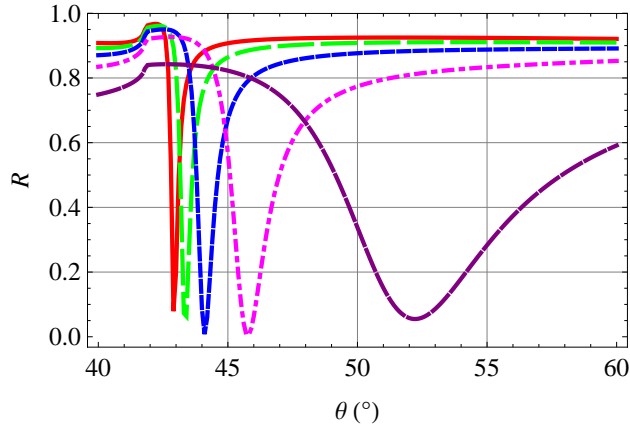


Fig. 11.5. Plot of the SP resonance as exhibited in the reflectivity of a 50 nm thin film of silver on a glass prism in the Kretschmann configuration in air as a function of angle of incidence, θ , for wavelengths of 800 nm (solid line), 700 nm (long dashes), 600 nm (short dashes), 500 nm (dot dashes), and 400 nm (medium dashes) . (*Mathematica* simulation.)

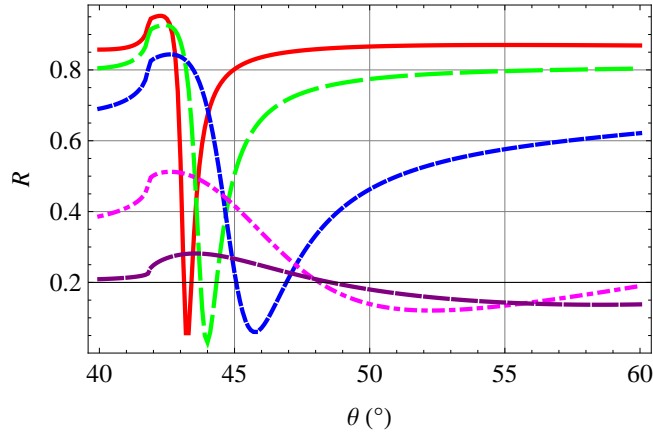


Fig. 11.6. Plot of the SP resonance as exhibited in the reflectivity of a 50 nm thin film of gold on a glass prism in the Kretschmann configuration in air as a function of angle of incidence, θ , for wavelengths of 800 nm (solid line), 700 nm (long dashes), 600 nm (short dashes), 500 nm (dot dashes), and 400 nm (medium dashes) . (*Mathematica* simulation.)

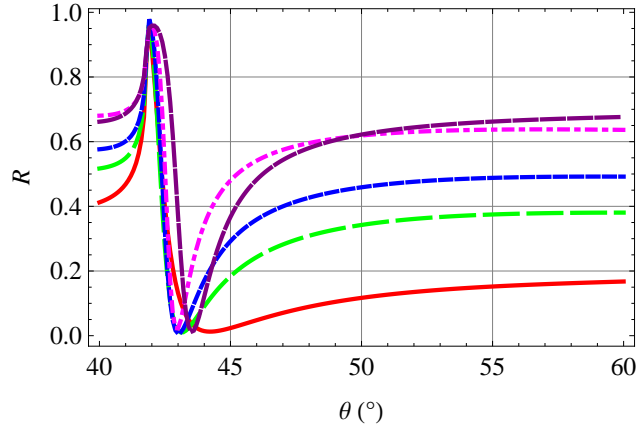


Fig. 11.7. Plot of the SP resonance as exhibited in the reflectivity of a thin film of aluminum on a glass prism in the Kretschmann configuration in air as a function of angle of incidence, θ . The thickness of the aluminum film is 7 nm at $\lambda = 800$ nm (solid line), 9 nm at $\lambda = 700$ nm (long dashes), 11 nm at $\lambda = 600$ nm (short dashes), and 15 nm at $\lambda = 400$ (medium dashes) and 500 nm (dot dashes). (*Mathematica* simulation.)

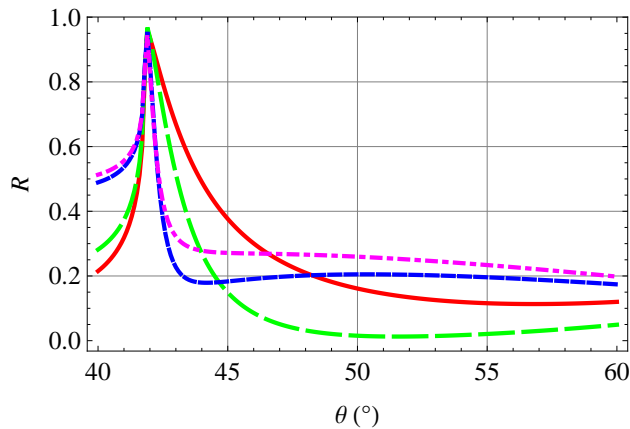


Fig. 11.8. Reflectivity for 10 nm films of iron (solid line), cobalt (long dashes), palladium (short dashes) and platinum (dot dashes) at a wavelength of 800 nm. There is no obvious SP resonance with a reflectivity minimum although there is still a strong reflectivity peak at the critical angle. (*Mathematica* simulation.)

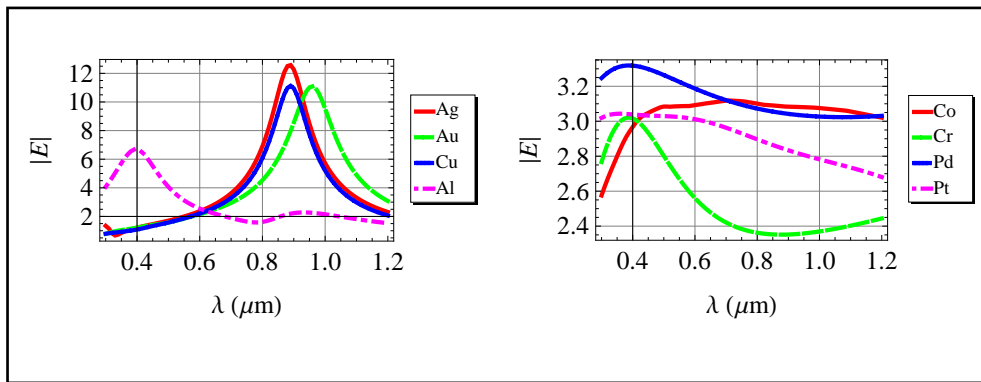


Fig. 11.9. Electric field amplitude as a function of wavelength, λ , for SP excitation in the Kretschmann configuration for several metals. The angle of incidence within the glass prism is 42.7° , except for aluminum for which it is 43.1° . The thicknesses of the films are adjusted for maximum field amplitude at the surface. (*Mathematica* simulation.)

11.2.3 Propagation distance

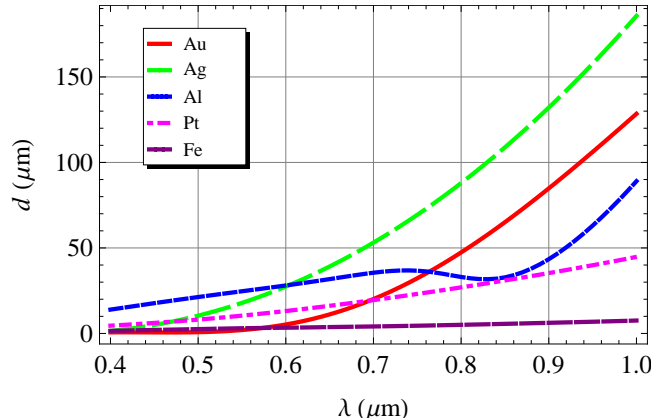


Fig. 11.10. SP propagation distance is plotted as a function of wavelength, λ , for gold (solid line), silver (long dashes), aluminum (short dashes), platinum (dot dashes) and iron (medium dashes). (*Mathematica* simulation.)

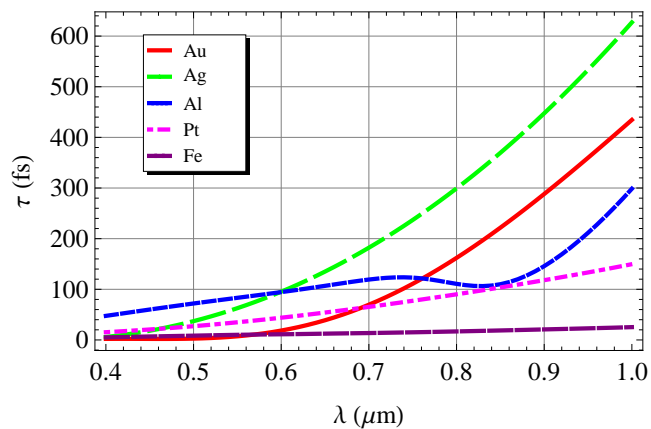


Fig. 11.11. SP lifetime is graphed as a function of wavelength, λ , for gold (solid), silver (long dashes), aluminum (short dashes), platinum (dot dashes) and iron (medium dashes). (*Mathematica* simulation.)

11.2.4 Nanoparticle field enhancement

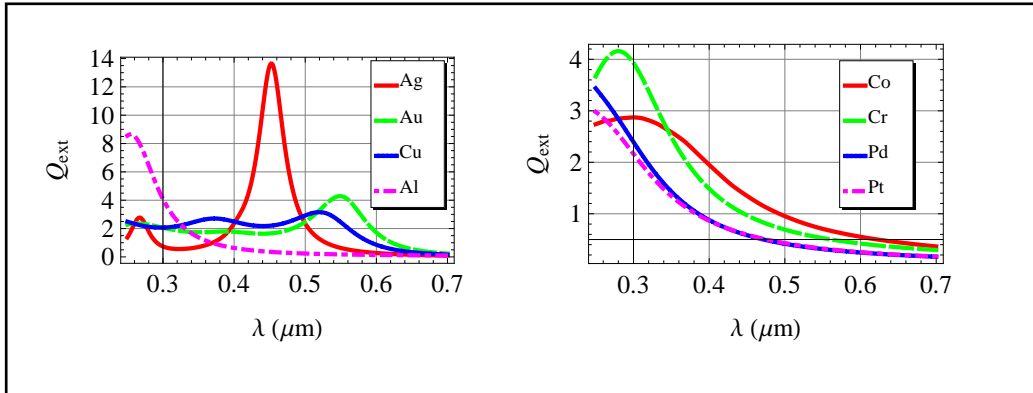


Fig. 11.12. Extinction coefficient as a function of wavelength for 40 nm particles of several metals embedded in a glass medium. Left: silver (solid line), gold (long dashes), copper (dots) and aluminum (dot dashes). Right: cobalt (solid line), chromium (long dashes), palladium (dots) and platinum (dot dashes). (*Mathematica* simulation.)

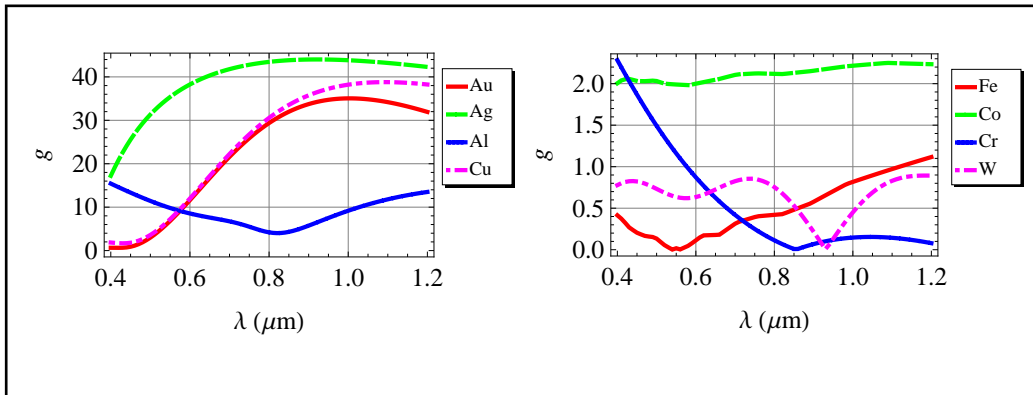


Fig. 11.13. Figure of merit as a function of wavelength for (left) plasmonic metals and (right) transition metals in the quasistatic approximation. Left: gold (solid line), silver (long dashes), aluminum (dots) and copper (dot dashes). Right: iron (solid line), cobalt (long dashes), chromium (dots) and tungsten (dot dashes). (*Mathematica* simulation.)

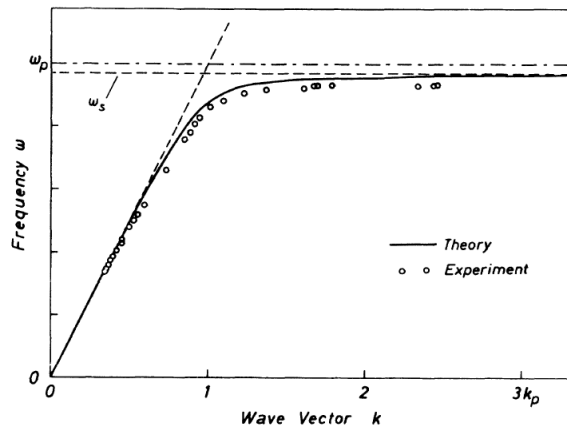


Fig. 11.14. SP dispersion curve for highly doped InSb. Reprinted with permission from N. Marschall, B. Fischer and H. J. Queisser, *Phys. Rev. Lett.* **27** 95 (1971). © 1971 by the American Physical Society. [8]

11.3 Drude metals

11.3.2 Lossless Drude model

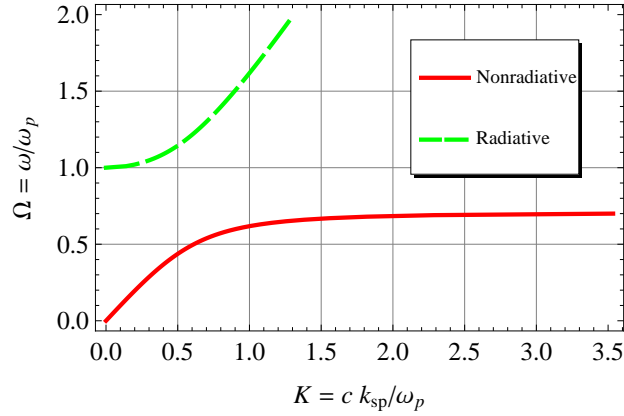


Fig. 11.15. SP dispersion curve for a Drude metal exhibiting two branches. (*Mathematica* simulation.)

Nonradiative SPs

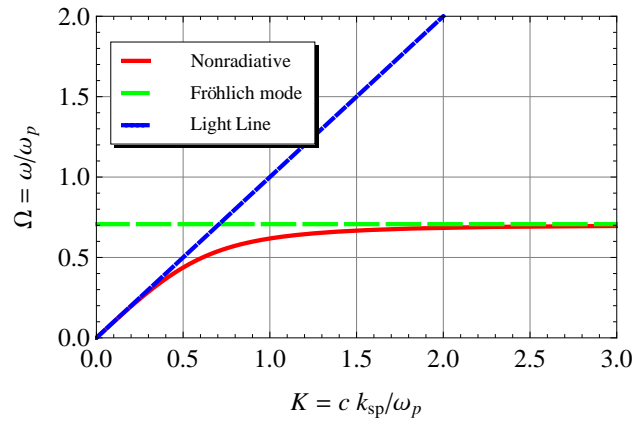


Fig. 11.16. Nonradiative lower branch of the SP dispersion curve for a Drude metal and its asymptotes. (*Mathematica* simulation.)

Radiative SPs

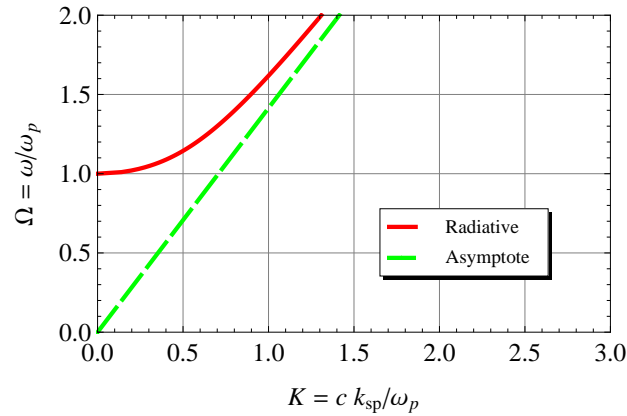


Fig. 11.17. Radiative upper branch of the SP dispersion curve for a Drude metal and its asymptote, which is the light line. (*Mathematica* simulation.)

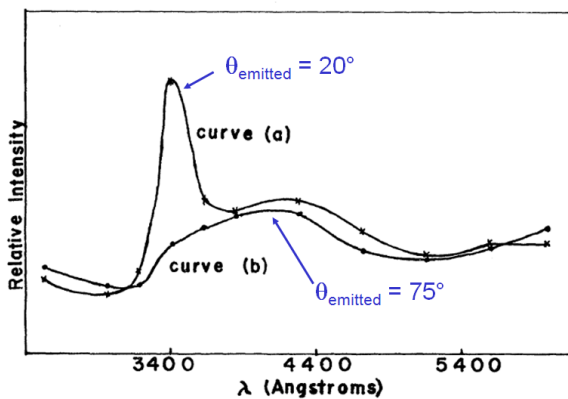


Fig. 11.18. Light emission from a thin silver film bombarded by electrons. Reprinted with permission from R. W. Brown, P. Wessel and E. P. Trounson, *Phys Rev. Lett.* **5** 472-473 (1960). © 1960 by the American Physical Society. [21]

11.3.3 Lossy Drude model

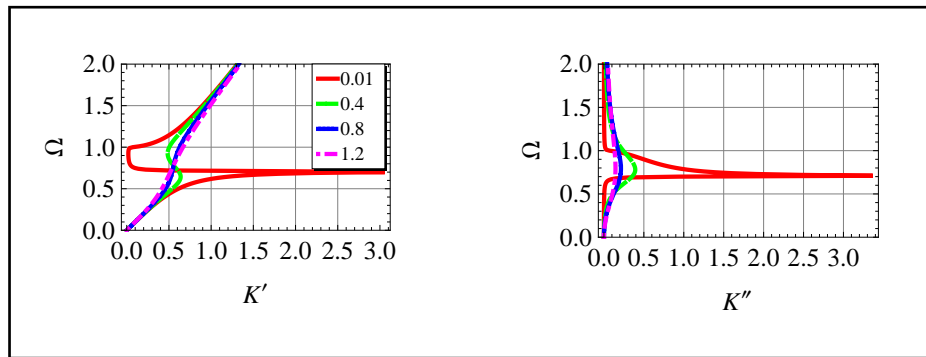


Fig. 11.19. Complex dispersion curves for SPs in a Drude metal assuming the frequency is real for damping constants of 0.01 (solid line), 0.4 (long dashes), 0.8 (dots) and 1.2 (dot dashes). (Left) SP frequency as a function of the real part of SP wavevector. (Right) SP frequency as a function of the imaginary part of SP wavevector. (*Mathematica* simulation).

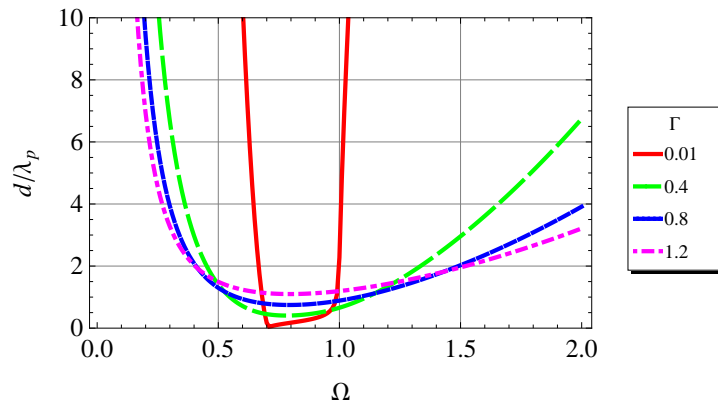
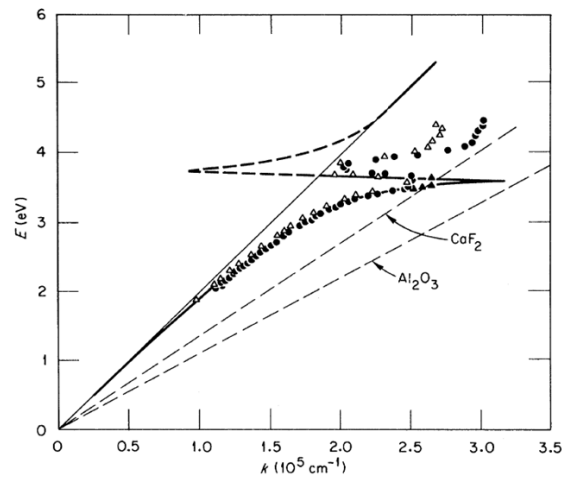


Fig. 11.20. Propagation distance for a SP in a lossy Drude metal as a function of frequency for damping constants of 0.01 (solid), 0.4 (long dashes), 0.8 (short dashes) and 1.2 (dot dashes). The propagation distance is normalized by the plasma wavelength, $\lambda_p = 2\pi c/\omega_p$. (*Mathematica* simulation.)



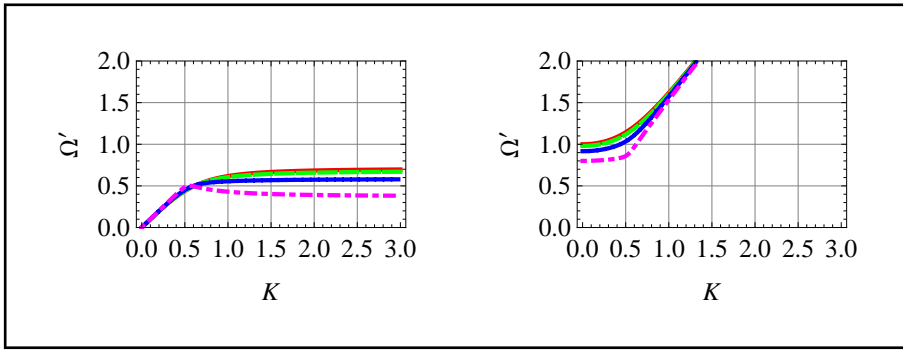


Fig. 11.22. Real part of the SP frequency as a function of SP wavevector for both the (left) lower and (right) upper branches of the dispersion curve for SPs in a Drude metal assuming the wavevector is real. The damping constant is 0 (solid line), 0.4 (long dashes), 0.8 (short dashes) and 1.2 (dot dashes). (*Mathematica* simulation.)

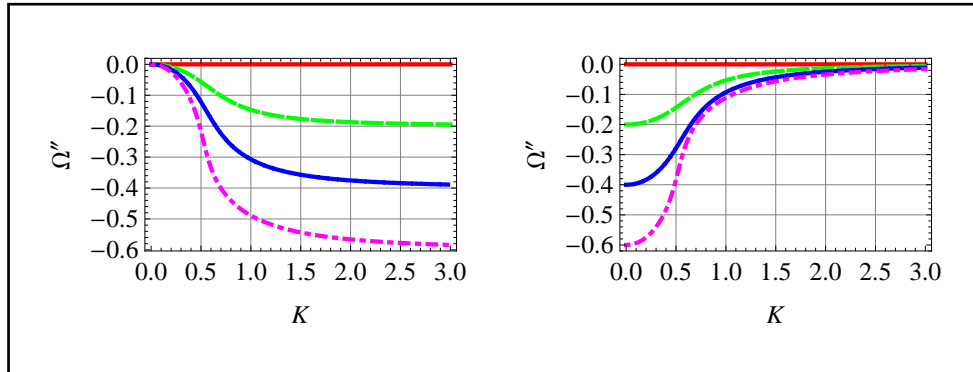
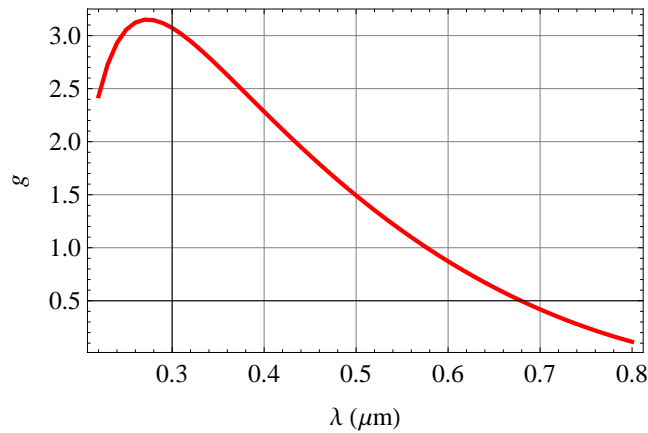


Fig. 11.23. Imaginary part of the SP frequency as a function of SP wavevector for both the (left) lower and (right) upper branches of the dispersion curve for SPs in a Drude metal assuming the wavevector is real. The damping constant is 0 (solid), 0.4 (long dashes), 0.8 (short dashes) and 1.2 (dot dashes). (*Mathematica* simulation.)

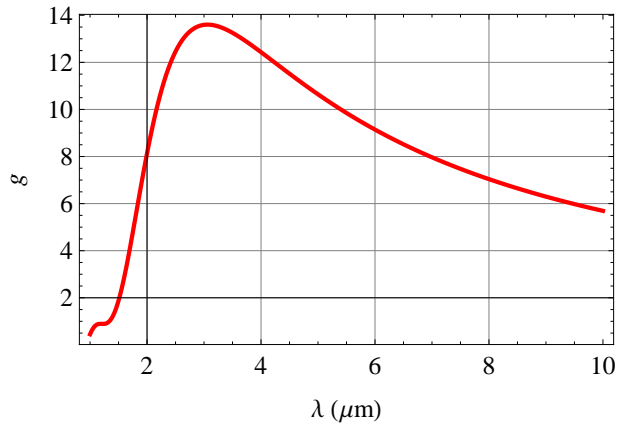
Exercises

1. In Fig. 11.11(b) the graph for chromium indicates an increasing field enhancement function at short wavelengths. Plot g for chromium from 250 nm to 800 nm. Does chromium become a plasmonic metal in the UV?



Exercise 1: Field enhancement factor for chromium. (*Mathematica* simulation.)

2. Tungsten is a highly resistive metal with a high melting point. These are properties that make it useful for heating elements and lamp filaments, but not useful for supporting SPs at optical frequencies as seen in Fig. 11(b). By plotting the field enhancement function from a wavelength of $1 \mu\text{m}$ to $10 \mu\text{m}$, decide whether or not this metal could support SPs at these longer IR wavelengths.



Exercise 2: Field enhancement factor for tungsten. (*Mathematica* simulation.)

References

- [1] J. R. Sambles, G. W. Bradbery and F. Yang. Optical excitation of surface plasmons: an introduction. *Contemp. Phys.* **32** (1991) 173.
- [2] O. Stephan, D. Taverna, M. Kociak, L. Henrard, K. Suenaga and C. Colliex. Surface plasmon coupling in nanotubes. In *Structural and Electronic Properties of Molecular Nanostructures*, ed. H. Kuzmany, J. Fink, M. Mehring and S. Roth. (New York: AIP, 2002), p. 477.
- [3] D. J. Nash and J. R. Sambles. Surface plasmon-polariton study of the optical dielectric function of silver. *J. Mod. Opt.* **43** (1996) 81.
- [4] R. A. Innes and J. R. Sambles. Optical characterisation of gold using surface plasmon-polaritons. *J. Phys. F: Met. Phys.* **17** (1987) 277.
- [5] M. D. Tillin and J. R. Sambles. A surface plasmon-polariton study of the dielectric constants of reactive metals: aluminum. *Thin Solid Films* **167** (1988) 73.
- [6] D. Y. Smith, E. Shiles and M. Inokuti. The optical properties of metallic aluminum. In *Handbook of Optical Constants of Solids*, ed. E. D. Palik. (San Diego: Academic Press, 1998), pp. 369.
- [7] M. van Exeter and A. Lagendijk. Ultrashort surface-plasmon and phonon dynamics. *Phys. Rev. Lett.* **60** (1988) 49.
- [8] N. Marschall, B. Fischer and H. J. Queisser. Dispersion of surface plasmons in InSb. *Phys. Rev. Lett.* **27** (1971) 95.
- [9] J. G. Rivas, M. Kuttge, P. H. Bolivar, H. Kurz and J. A. Sánchez-Gil. Propagation of surface plasmon polaritons on semiconductor gratings. *Phys. Rev. Lett.* **93** (2004) 256804.
- [10] A. S. Barker, Jr. Direct optical coupling to surface excitations. *Phys. Rev. Lett.* **28** (1972) 892.
- [11] A. Dereux, J-P. Vigneron, P. Lambin and A. A. Lucas. Polaritons in semiconductor multilayered materials. *Phys. Rev. B* **38** (1988) 5438.

- [12] D. J. Nash and J. R. Sambles. Surface plasmon-polariton study of the optical dielectric function of copper. *J. Mod. Opt.* **42** (1995) 1639.
- [13] T. Kloos and H. Raether. The dispersion of surface plasmons of Al and Mg. *Phys. Lett.* **44A** (1973) 157.
- [14] M. D. Tillin and J. R. Sambles. Surface plasmon-polariton study of the dielectric function of magnesium. *Thin Solid Films* **172** (1989) 27.
- [15] G. J. Kovacs. Optical excitation of surface plasma waves in an indium film bounded by dielectric layers. *Thin Solid Films* **60** (1979) 33.
- [16] M. G. Blaber, M. D. Arnold, N. Harris, M. J. Ford and M. B. Cortie. Plasmon absorption in nanospheres: a comparison of sodium, potassium, aluminium, silver and gold. *Physica B: Cond. Mat.* **394** (2007) 184.
- [17] H. J. Simon, D. E. Mitchell and J. G. Watson. Second harmonic generation with surface plasmons in alkali metals. *Opt. Commun.* **13** (1975) 294.
- [18] Y. Xiong, J. Chen, B. Wiley, Y. Xia, Y. Yin and Z-Y. Li. Size-dependence of surface plasmon resonance and oxidation for Pd nanocubes synthesized via a seed etching process. *Nano Letters* **5** (2005) 1237.
- [19] N. Zettsu, J. M. McLellan, B. Wiley, Y. Yin, Z-Y. Li and Y. Xia. Synthesis, stability, and surface plasmonic properties of rhodium multipods, and their use as substrates for surface-enhanced Raman scattering. *Ang. Chem. - Intern. Ed.* **45** (2006) 1288.
- [20] F. Yang, G. W. Bradberry and J. R. Sambles. Study of the optical properties of obliquely evaporated nickel films using IR surface plasmons. *Thin Solid Films* **196** (1991) 35.
- [21] R. W. Brown, P. Wessel and E. P. Trounson. Plasmon radiation from silver films. *Phys Rev. Lett.* **5** (1960) 472.
- [22] R. A. Ferrell. Predicted radiation of plasma oscillations in metal films. *Phys. Rev.* **111** (1958) 1214.

- [23] E. T. Arakawa, M. W. Williams, R. N. Hamm and R. H. Ritchie. Effect of damping on surface plasmon dispersion. *Phys. Rev. Lett.* **31** (1973) 1127.